ASTRONOMY & ASTROPHYSICS
SUPPLEMENT SERIES

Astron. Astrophys. Suppl. Ser. **137**, 351–362 (1999)

Understanding A-type supergiants

I. Ultraviolet and visible spectral atlas⋆ of A-type supergiants⋆⋆

E. Verdugo[1], **A. Talavera**[2], **and A.I. Gómez de Castro**[3]

[1] ISO Data Centre, P.O. Box 50727, E-28080-Madrid, Spain
e-mail: everdugo@iso.vilspa.esa.es
[2] LAEFF/INTA, P.O. Box 50727, E-28080-Madrid, Spain
e-mail: ati@laeff.esa.es
[3] Instituto de Astronomía y Geodesia (CSIC-UCM), Fac. cc. Matemáticas, Universidad Complutense, Av. Complutense s/n, E-28040-Madrid, Spain
e-mail: aig@orion.mat.ucm.es

Received October 14, 1997; accepted April 12, 1999

Abstract. This paper is the first of a series whose aim is to perform a systematic study of A-type supergiant atmospheres and winds. Here we present a spectral atlas of 41 A-supergiants observed by us in high and medium resolution in the visible and ultraviolet. The atlas consists of profiles of the Hα, Hβ, Hγ, Hδ, Hϵ, Ca II (H and K), Na I (D1 and D2), Mg II$_{4481}$, Mg II [uv1] and Fe II [uv1, uv2, uv3, uv62, uv63, uv161] lines for 41 stars with spectral types ranging from B9 to A9 and luminosity classes Ia, Iab and Ib, and provides the basic data for a thoughtful study of these stars. The overall characteristics of the sample as well as the data reduction procedures are described. We also present some examples of spectral variability.

Key words: atlases — line: profiles — stars: supergiants — ultraviolet: stars

1. Introduction

Mass loss is ubiquitous among highly luminous OBA stars. The last decade has seen an enormous increase in the number and the quality of the observational studies of stellar winds. At the same time the theory of stellar winds has been improved dramatically. However most of this work has been limited to O and B stars. To date, very few studies have been devoted to A-type supergiants. These stars occupy a region of the HR diagram where evolution is rapid and therefore they are few in number. Furthermore, the indicators of stellar winds are significantly weaker in A-supergiants than in OB supergiants. Nevertheless it is known from the few A supergiants studied that the structure of their stellar wind is unique in some way that is not yet understood.

There are no comprehensive studies of the line profiles formed in the winds of these stars, of which only a few have been studied in detail. In the optical, a photographic survey of Hα emission in luminous O9 to A5 stars was undertaken by Rosendhal (1973) showing the strong influence of luminosity upon the Hα profile in late-B and A supergiants. The emission at Hα disappears for stars fainter than absolute visual magnitude -6.8 to -7.0, while at the highest luminosities emission dominates over absorption. In the ultraviolet, where most of the indicators of mass loss are observed, the UV P Cygni profiles for O and early B stars have been studied by a large number of authors. However the UV spectra of A-supergiants have scarcely been examined (e.g. Lamers et al. 1995; Lamers et al. 1978; Praderie et al. 1980; Underhill & Doazan 1982; Hensberge et al. 1982); the most extensive study was performed by Talavera & Gómez de Castro (1987) from the high resolution data available in the International Ultraviolet Explorer (IUE) satellite archive. They found two different groups of A-supergiants: stars showing spectral lines characteristic of mass outflow and stars which do not show any sign of stellar winds in their spectrum. The mass-losing

Send offprint requests to: E. Verdugo

⋆ Figures 1-3 are only available in electronic form at the http://www.edpsciences.com

⋆⋆ Based on observations made with the INT and JKT telescopes operated on the island of La Palma by the RGO in the Spanish Observatorio del Roque de Los Muchachos of the Instituto de Astrofisica de Canarias, with the 2.2 m telescope at Calar Alto Observatory, Spain, with the Bernard Lyot 2 m telescope at Pic Du Midi Observatory, France and observations collected at the European Southern Observatory at La Silla, Chile.

Table 1. Basic properties of the program stars

Star		*Position (2000.0)*		m_v	M_v	*OB Assoc.*	*Available data*	
HD/BD	Other name	α	δ				Visible	IUE
BD +60 51	SAO 11196	00 26 33.7	+61 24 46	9.23	−4.80	Cas OB4	Y	N
HD 2928	SAO 11258	00 33 13.3	+62 32 14	8.61	−5.50	Cas OB4	Y	Y
HD 3940	SAO 11343	00 42 50.0	+64 17 28	7.26	−6.37	Cas OB7	Y	Y
BD +61 153	SAO 11344	00 42 59.1	+62 14 06	9.32	−4.69	Cas OB7	Y	N
HD 4717	SAO 11421	00 50 16.1	+63 10 17	8.9	−5.90	Cas OB7	Y	N
HD 5776	SAO 11519	01 00 32.8	+63 01 44	8.05	−4.97	Cas OB7	Y	Y
HD 12953	V472 Per	02 08 40.4	+58 25 25	5.67	−7.81	Per OB1	Y	Y
HD 13476	HR 641	02 13 41.5	+58 33 39	6.44	−7.10	Per OB1	Y	Y
HD 13744	SAO 23101	02 15 58.5	+58 17 37	7.59	−6.46	Per OB1	Y	Y
HD 14433	SAO 23243	02 21 55.3	+57 14 34	6.39	−6.89	Per OB1	Y	Y
HD 14489	i Per	02 22 21.3	+55 50 44	5.20	−7.84	Per OB1	Y	Y
HD 14535	SAO 23263	02 22 53.4	+57 14 42	7.44	−6.50	Per OB1	Y	Y
HD 15316	SAO 23374	02 29 58.6	+57 49 15	7.23	−6.48	Per OB1	Y	Y
HD 16778	SAO 23564	02 43 53.5	+59 49 22	7.71	−6.89	Per OB1	Y	Y
HD 236995	SAO 23582	02 45 03.4	+58 33 05	8.63	−4.77	Per OB1	Y	N
HD 17378	V480 Per	02 49 30.6	+57 05 03	6.25	−7.81	Per OB1	Y	Y
HD 20041	HR 964	03 15 47.9	+57 08 26	5.79	−6.60	Cam OB1	Y	Y
HD 21389	HR 1040	03 29 54.7	+58 52 43	4.54	−7.10	Cam OB1	Y	Y
HD 46300	13 Mon	06 32 54.2	+07 19 59	4.50	−4.80	Mon OB1	Y	Y
HD 59612	HR 2874	07 29 51.4	−23 01 28	4.85	−5.10	-	Y	Y
HD 87737	η Leo	10 07 19.9	+16 45 45	3.52	−5.30	Sco-Cen	N	Y
HD 92207	V370 Car	10 37 27.0	−58 43 60	5.46	−8.00	Car OB1	N	Y
HD 100198	V809 Cen	11 31 15.0	−61 16 42	6.31	−7.20	Car-Cen	N	Y
HD 100826	SAO 251469	11 35 42.3	−61 17 16	6.29	−5.40	NGC 3766	N	Y
HD 102878	HR 4541	11 50 27.2	−62 38 57	5.70	−7.00	Cru OB1	Y	Y
HD 103516	HR 4563	11 54 59.9	−63 16 44	5.90	−4.90	Car-Cen	N	Y
HD 104035	HR 4578	11 58 47.7	−64 20 21	5.61	−5.20	Car-Cen	N	Y
HD 104111	SAO 251670	11 59 25.6	−62 49 51	6.37	-	-	N	Y
HD 161912	iot02 Sco	17 50 11.0	−40 05 25	4.81	−4.70	-	N	Y
HD 187983	HR 7573	19 52 01.4	+24 59 32	5.57	−6.50	Vul OB4	Y	N
HD 197345	α Cyg	20 41 25.8	+45 16 49	1.25	−8.55	Cyg OB7	Y	Y
HD 207260	ν Cep	21 45 26.9	+61 07 15	4.30	−6.82	Cep OB2	Y	Y
HD 207673	HR 8345	21 49 40.0	+41 08 56	6.48	−4.97	-	Y	Y
HD 209900	SAO 34034	22 05 13.7	+53 30 37	8.71	−4.85	Cep OB1	Y	N
HD 210221	HR 8443	22 07 25.5	+53 18 27	6.14	−5.00	Cep OB1	Y	Y
HD 211971	SAO 34314	22 19 25.6	+60 08 52	6.90	−5.50	Cep OB2	Y	Y
HD 212593	4 Lac	22 24 30.9	+49 28 35	4.56	−5.86	Lac OB1	Y	Y
HD 213470	SAO 34531	22 30 18.6	+57 13 32	6.65	−7.09	Cep OB1	Y	Y
BD +60 2542	SAO 20639	23 27 05.6	+61 22 42	8.82	−5.09	Cas OB2	Y	N
HD 223385	6 Cas	23 48 50.1	+62 12 52	5.43	−8.22	Cas OB5	Y	Y
HD 223960	SAO 20923	23 53 49.9	+60 51 13	6.93	−6.90	Cas OB5	Y	Y

Note: Y ≡ Observed.
N ≡ Not observed.

stars showed absorption shortward shifted components in the Mg II, Fe II, C II, Si II and Al II lines. Moreover these components are variable, as well as the terminal velocity measured from the violet edge of the resonance Mg II lines. Contrary to the relation found by Abbot (1978) for radiatively driven winds in OB supergiants, Talavera & Gómez de Castro (1987) found that the measured terminal velocity in A-supergiants decreases as the escape velocity increases. Therefore the radiation driven wind theory seems to be not applicable to A-supergiants. However, the latest theoretical progress on this point (Achmad et al. 1997; McCarthy et al. 1997; Kudritzki et al. 1997) has begun to clarify such discrepancies in the radiatively driven wind theory frame.

Mass loss from early type stars is due to radiation pressure on UV lines, although a detailed comparison of the predicted and observed mass loss rates of OB stars shows

Table 2. Spectral types

Star	Spectral Type from different sources						
	(Hu)	(GS)	(Bw)	(Fn)	(KG)	(Cz)	(St)
BD+60 51	A2 Ib						
HD 2928	A0 Iab						
HD 3940	A1 Ia	A1 Ia					
BD+61 153	A0 Ib	A0 Ib					
HD 4717	A0 Ib						
HD 5776	A0 Ib	A0 Ib					
HD 12953	A1 Ia	A1 Ia		A1 Ia			
HD 13476	A3 Iab	A3 Iab	A3 Iab				
HD 13744	A0 Iab	A0 Iab	B9 Iab				
HD 14433	A1 Ia	A1 Ia					
HD 14489	A2 Ia	A2 Iabs	A3 Ia				
HD 14535	A2 Iap	A2 Iabs					
HD 15316	A3 Iab	A2 Ia	A2 Iab				
HD 16778	A2 Ia	A2 Ia	A1 Ia				
HD 236995	A0 Ib	A0 Ib					
HD 17378	A5 Ia	A5 Ia	A3 Ia-Iab				
HD 20041	A0 Ia		B9.5 Ia				
HD 21389	A0 Ia		A0 Ia				
HD 46300	A0 Ib	A0 Ib	A1 Ib	A0 Ib			
HD 59612	A5 Ib		A5 Ib-II	A5 Ib			
HD 87737	A0 Ib		A0 Iab	A0 Ib			
HD 92207	A0 Ia			A0 Ia			
HD 100198				A3 Ia			
HD 100826				A0 Ia			A0 Ib
HD 102878	A2 Ia-Iab				A2 Ia		
HD 103516	A3 Ib			B9 II			
HD 104035	A3 Ib			A3 Ib			
HD 104111				A9 Ib/II			
HD 161912	A2 Ib						
HD 187983	A1 Iab			A1 Iab			
HD 197345	A2 Ia	A2 Ia	A0 Ia				
HD 207260	A2 Iab	A2 Ia	A5 Ia				
HD 207673			A1 Iab			A2 Ib	
HD 209900	A0 Ib	A0 Ib					
HD 210221			A3 Ib				
HD 211971	A2 Ib		A1 Ia				
HD 212593	B9 Iab		B9 Ia				
HD 213470	A3 Ia	A3 Ia	A3 Ia				
BD+60 2542	A2 Ib	A2 Ib					
HD 223385	A3 Ia	A3 Ia					
HD 223960	A0 Ia +	A0 Ia+					

References:
(Hu) Humphreys (1978).
(GS) Garmany & Stencel (1992).
(Bw) Bouw (1981).
(St) Stothers (1991).
(Fn) Fernie (1983).
(KG) Kaltcheva & Georgiev (1994).
(Cz) Cananzi et al. (1993).

systematic differences. Such a comparison has not been made for A-supergiants. Moreover for the few studied, the mass loss rates derived from the UV lines are significantly lower, by a factor 10^{-1} to 10^{-2}, than the rates derived from Hα (Praderie et al. 1980; Hensberge et al. 1982; Kunasz & Morrison 1982). Another source of discrepancy is the problem of the superionization of the wind of early-type stars (Lamers & Snow 1978; Cassinelli et al. 1978; Groenewegen & Lamers 1991; Owocki 1992). There is as yet no study of the presence or absence of superionization in the winds of A supergiants.

We have selected 41 A-type supergiants to carry out a systematic study of stellar wind indicators in these stars in the visible and ultraviolet. In this atlas we show the profiles of the Hα, Hβ, Hγ, Hδ, Hϵ Balmer lines, the Ca II H and K lines, the Na I D lines, Mg II$_{4481}$, Mg II [uv1] and Fe II [uv1, uv2, uv3, uv62, uv63, uv161] for the program stars, as well as some relevant examples of the variations in the profiles.

The A-supergiants sample is presented in Sect. 2. The observations and the data reduction techniques are described in Sect. 3. The spectral atlas is introduced in Sect. 4 and a brief summary is provided in Sect. 5.

A detailed analysis of these data and their implications for the understanding of A-type supergiants will be published in a series of forthcoming papers (Verdugo et al. 1999).

2. The program stars

The stars selected belong to OB associations or clusters, so that we have a good estimate of the distance and therefore of the absolute magnitude. We have used the catalogue of Garmany & Stencel (1992) which is largely based on the cluster distances obtained by Humphreys (1978). In these catalogues the sample is biased towards early A-type supergiants. We have tried hard to get a good sample of all the luminosity classes for each spectral type since we expect significant luminosity effects in the lines formed in the wind. The whole sample is listed in Table 1; ordered by right ascension and identified by their entry number in the HD or BD catalogues. Another usual identification (as the SAO number or the variable star name) is provided in the second column. The equatorial coordinates (α(2000.0), δ(2000.0)) are given in the third and fourth column. The apparent visual magnitudes are listed in the fifth column. The absolute visual magnitude and the OB associations to which each of the stars belongs are given in the sixth and seventh columns respectively. The absolute magnitudes come from the catalogues cited above and they are calculated from the adopted distance to the association.

Most of the stars have been observed both in the ultraviolet and visible, although the less luminous stars could not be observed with the IUE satellite and only two southern stars were observed in the visible. We summarize this information in the last two columns of Table 1.

Table 3. Observed spectral ranges

Campaign	Central λ (Å)	$\Delta\lambda$ (Å)	Dispersion (Å/pixel)
La Palma (INT)	3951	96	0.166
	4481	97	0.168
	5889	62	0.107
	6563	100	0.173
La Palma (JKT)	4300	400	0.39
	4800	350	0.34
	6200	650	0.63
	6678	820	0.80
Calar Alto (2.2 m)	3950	131	0.128
	4481	133	0.130
	4861	132	0.129
	5889	124	0.121
	6562	100	0.097

In Table 2 we give the tabulated spectral types of each star taken from the literature (Humphreys 1978; Garmany & Stencel 1992; Bouw 1981; Fernie 1983; Stothers 1991; Kaltcheva & Georgiev 1994; Cananzi et al. 1993).

3. Observations and data reduction

3.1. Visible data

3.1.1. Observations

We have carried out four different visible campaigns to observe the Hα, Hβ, Hγ, Hδ and Hϵ Balmer lines, Ca II H and K, Na I D and Mg II λ 4481 Å lines. The observed spectral ranges are listed in Table 3. We summarize in Table 4 the information available for each star as well as the instrumental set-up (telescope+spectrograph) used to obtain the data and the Julian date of the observations.

The first campaign was carried out in September 1988 with the Isaac Newton Telescope of the Roque de los Muchachos Observatory in La Palma. All the spectra were taken with the Intermediate Dispersion Spectrograph (IDS) equipped with a GEC CCD which has 22 μm pixels arranged in an 578 × 385 array. We observed Hα, Ca II H and K, Na I D and the Mg II$_{4481}$ lines with a resolving power around 16 500.

The second campaign (October 1988) was carried out with the Coudé Spectrograph (resolving power around 26 000) of the 2.2 m telescope at the Calar Alto Observatory. The detector used was an RCA CCD (1024 × 656, 15 μ pixels). We obtained the Hα, Hβ, Ca II(H, K) and Mg II$_{4481}$ profiles.

The third campaign was carried out in the Pic Du Midi Observatory (France) in August 1994. We used the MUSICOS (for **MU**lti-**SI**te **CO**ntinuous **S**pectroscopy)

Table 4. Journal of observations in the visible

STAR	Sp. Range	Tel.	JD-2440000.	STAR	Sp. Range	Tel.	JD-2440000.
BD +60 51	Hα	INT	7432.45, 7434.45	HD 14433	Hα	INT	7431.63, 7433.67
	NaI+HeI	INT	7433.57			CA	7458.56
	MgII+HeI	INT	7431.54			JKT	9614.65, 9615.61
HD 2928	Hα	INT	7432.48, 7434.47		CaII	INT	7432.67
		JKT	9615.55			CA	7454.55
	NaI+HeI	INT	7433.59		NaI+HeI	INT	7434.66
	Hβ	CA	7458.48		Hβ	CA	7456.55
	MgII+HeI	CA	7457.46			JKT	9616.62
HD 3940	Hα	INT	7432.50, 7434.50		MgII+HeI	INT	7434.71
		CA	7458.45	HD 14489	Hα	INT	7431.64, 7433.68
		JKT	9614.61, 9615.54			CA	7458.57
	NaI+HeI	INT	7433.61			JKT	9614.66, 9615.61
	Hβ	CA	7458.47		CaII	INT	7432.70
		JKT	9616.55		NaI+HeI	INT	7434.67
	MgII+HeI	CA	7457.50			JKT	9621.71
	Hγ + Hδ	JKT	9621.55		Hβ	CA	7456.56
BD +61 153	Hα	INT	7432.51, 7434.50			JKT	9616.63
	NaI+HeI	INT	7433.62		MgII+HeI	INT	7434.73
	MgII+HeI	INT	7431.56		Hγ + Hδ	JKT	9621.59
HD 4717	Hα	INT	7432.53, 7434.53	HD 14535	Hα	INT	7432.58, 7434.56
	NaI+HeI	INT	7434.62			CA	7458.58
	MgII+HeI	CA	7457.51			JKT	9614.66, 9615.62
HD 5776	Hα	INT	7432.56, 7434.55		NaI+HeI	INT	7434.67
	NaI+HeI	INT	7434.63			JKT	9621.72
	Hβ	CA	7458.51		Hβ	CA	7456.56
	MgII+HeI	CA	7457.54			JKT	9616.64
HD 12953	Hα	INT	7431.62, 7433.65		MgII+HeI	CA	7457.58
		CA	7455.52		Hγ + Hδ	JKT	9621.60
		JKT	9614.62, 9615.59	HD 15316	Hα	INT	7432.59, 7434.57
	CaII	INT	7432.66			CA	7458.59
		CA	7452.55, 7454.52			JKT	9614.67, 9615.64
	NaI+HeI	INT	7434.64		NaI+HeI	INT	7434.69
		CA	7460.71		Hβ	CA	7456.58
	MgII+HeI	INT	7434.70			JKT	9616.66
	Hβ	CA	7456.52		MgII+HeI	CA	7457.60
		JKT	9616.58	HD 16778	Hα	INT	7432.60, 7434.58
HD 13476	Hα	INT	7431.64, 7433.66			JKT	9614.68, 9615.65
		CA	7458.54		NaI+HeI	INT	7434.61
		JKT	9614.63, 9615.60			JKT	9621.73
	NaI+HeI	INT	7434.65		Hβ	CA	7456.60
		JKT	9621.71			JKT	9616.67
	Hβ	CA	7456.52		MgII+HeI	CA	7457.61
		JKT	9616.59	HD 17378	Hα	INT	7431.66, 7433.68
	MgII+HeI	CA	7457.56			CA	7455.66
	Hγ	JKT	9621.58			JKT	9614.69, 9615.68
HD 13744	Hα	INT	7431.65, 7433.66		NaI+HeI	INT	7433.62
		CA	7458.55		CaII	INT	7432.70
		JKT	9614.64, 9615.60			CA	7452.59, 7454.60
	NaI+HeI	INT	7434.66		Hβ	CA	7456.64
	Hβ	CA	7456.53			JKT	9616.70
		JKT	9616.60		MgII+HeI	INT	7434.74
	MgII+HeI	CA	7457.57		Hγ + Hδ	JKT	9621.62

Note: INT = Isaac Newton Telescope + IDS;
CA = 2.2 m Telescope, Calar Alto + Coudé;
JKT = Jacobus Kapteyn Telescope + RBS.

Table 4. continued

STAR	Sp. Range	Tel.	JD-2440000.	STAR	Sp. Range	Tel.	JD-2440000.
HD 20041	Hα	INT	7432.63, 7434.59	HD 210221	Hα	INT	7432.37, 7434.38
		CA	7455.65			CA	7458.34
		JKT	9614.69, 9615.68			JKT	9614.45
	NaI+HeI	INT	7433.76, 7434.60		NaI+HeI	INT	7433.52
		JKT	9621.73		CaII	CA	7452.39
	CaII	CA	7457.68		Hβ	CA	7456.36
	Hβ	CA	7456.65			JKT	9616.47
		JKT	9616.70	HD 211971	Hα	INT	7432.38, 7434.38
	MgII+HeI	CA	7457.66		NaI+HeI	INT	7433.53
	Hγ + Hδ	JKT	9621.64			JKT	9621.40
HD 21389	Hα	INT	7431.67, 7433.70		CaII	CA	7455.39
		CA	7455.64		Hβ	CA	7456.37
		JKT	9614.70, 9615.69			JKT	9616.48
	NaI+HeI	INT	7433.73		MgII+HeI	INT	7433.37
		JKT	9621.74		Hγ + Hδ	JKT	9618.51
	CaII	INT	7432.72	HD 212593	Hα	INT	7432.38
		CA	7452.64			CA	7458.35
	Hβ	CA	7456.66			JKT	9614.48
		JKT	9616.72		NaI+HeI	INT	7433.53
	MgII+HeI	INT	7432.77		CaII	CA	7454.38
HD 46300	Hα	INT	7431.68, 7433.71		Hβ	CA	7456.38
		CA	7455.69			JKT	9616.49
	NaI+HeI	INT	7433.72		MgII+HeI	INT	7433.38
	CaII	INT	7432.73	HD 213470	Hα	INT	7432.39, 7434.40
		CA	7452.72			CA	7458.36
	Hβ	CA	7456.66			JKT	9614.50, 9615.48
	MgII+HeI	INT	7432.76		NaI+HeI	INT	7433.54
	Hγ + Hδ	JKT	9617.74			JKT	9621.40
HD 187982	Hα	JKT	9614.44, 9614.51		CaII	CA	7457.32
	NaI+HeI	JKT	9621.36		Hβ	CA	7456.39
	Hβ	JKT	9616.41			JKT	9616.50
HD 197345	Hα	INT	7432.33, 7434.35		MgII+HeI	INT	7433.39
		JKT	9614.36		Hγ + Hδ	JKT	9621.45
	NaI+HeI	INT	7433.50	BD +60 2542	Hα	INT	7432.40, 7434.41
		JKT	9621.37			JKT	9614.57
	CaII	INT	7433.46		NaI+HeI	INT	7433.54
		CA	7452.35, 7455.36		CaII	CA	7457.34
	Hβ	CA	7456.30		Hβ	CA	7456.40
		JKT	9616.39		MgII+HeI	CA	7457.37
	MgII+HeI	INT	7433.34	HD 223385	Hα	INT	7432.44
HD 207260	Hα	INT	7432.33, 7434.35			CA	7458.38
		CA	7458.33		NaI+HeI	INT	7433.56
		JKT	9614.36, 9615.42			CA	7456.48
	NaI+HeI	INT	7433.50			JKT	9621.42
		JKT	9621.38		CaII	INT	7433.45
	CaII	INT	7433.44			CA	7454.40
		CA	7452.36		Hβ	CA	7456.42
	Hβ	CA	7456.34		MgII+HeI	CA	7457.39
		JKT	9616.42		Hγ + Hδ	JKT	9621.51
	MgII+HeI	INT	7433.35				
	Hγ + Hδ	JKT	9618.47				
HD 207673	Hα	JKT	9614.43, 9614.52				
	NaI+HeI	JKT	9621.39				
	Hβ	JKT	9616.43				
	Hγ + Hδ	JKT	9618.47				

Table 4. continued

STAR	Sp. Range	Tel.	JD-2440000.	STAR	Sp. Range	Tel.	JD-2440000.
HD 209900	Hα	INT	7432.34, 7434.35	HD 223960	Hα	INT	7432.44, 7434.44
		JKT	9614.41			CA	7458.44
	NaI+HeI	INT	7433.51			JKT	9614.65, 9615.53
	CaII	CA	7457.29		NaI+HeI	INT	7433.57
	Hβ	CA	7458.29			JKT	9621.42
		JKT	9616.44		CaII	INT	7433.46
	MgII+HeI	INT	7433.40			CA	7454.43
					Hβ	CA	7448.31
						JKT	9616.54
					MgII+HeI	INT	7431.52
					Hγ + Hδ	JKT	9621.47

Spectrograph (Baudrand & Böhm 1992) coupled to the 2 m Bernard Lyot Telescope (TBL) by means of a double optical fiber of 50 μm core diameter (due to the mechanical separation of the spectrograph from the telescope, excellent stability is guaranteed during the night). The MUSICOS spectrograph works in cross-dispersion mode allowing the observation of whole visible range (from 380 nm to 880 nm) in two exposures with a resolving power around 38 000. Six stars of our sample were observed with this instrument.

The last campaign was carried out in September 1994 with the Jacobus Kapteyn Telescope of the Roque de los Muchachos Observatory in La Palma. We used the Richardson Brealey Spectrograph (RBS) with a TEK CCD which has 24 μm pixels arranged in a 1024×1024 array. In this campaign we paid special attention to the Hγ and Hδ lines which were observed simultaneously with a resolving power around 3700.

The spectra of the two southern stars (HD 59612 and HD 102878) were kindly provided to us by Andreas Kaufer. These spectra were taken in La Silla with the Heidelberg Extended Range Optical Spectrograph (HEROS) at the ESO 50 cm telescope. HEROS is a portable fibre-linked two-channel echelle spectrograph which covers from 345 nm to 560 nm and from 580 nm to 865 nm in one exposure. The resolving power is around 20 000 over the complete wavelength range and, as with MUSICOS, stability is guaranteed by the separation from the telescope.

3.1.2. Reduction

The spectra obtained at La Palma and Calar Alto have been processed using standard astronomical data reduction packages (IHAP (Middelburg 1981), MIDAS[1] and IRAF[2]). In all cases the spectra have been extracted from the CCD frame after dark noise correction and flatfielding. At this stage, each spectrum was rebinned into a wavelength scale by using a polynomial fit to the positions provided by the comparison lamps (ThAr, ThNe or CuNe). A calibration spectrum was obtained immediately after the stellar spectrum, without any change in the spectrograph configuration. The long-term accuracy achieved for the wavelength calibration is of the order of 1 km s^{-1}.

In the final step the resulting wavelength-calibrated spectrum was rebinned to heliocentric velocities and the continuum was normalized to unity by fitting a low-order polynomial and dividing the spectrum by this function.

The MUSICOS spectra were semi-automatically reduced with the dedicated software MUSBIC. A complete description of this procedure can be found in Baudrand & Böhm (1992). Briefly, as the acquisition, the reduction is divided into two spectral domains: the red ($550-890$ nm) and the blue ($390-550$ nm). Both domains are precisely defined with regard to the order positions. The first step carried out by the program is to determine the exact position of the orders. The procedure is performed on the stellar, flatfield and calibration spectra. Then the program extracts each order of these spectra. The half-widths of the nearly Gaussian order profiles (perpendicular to the dispersion) vary between 2.5 and 3.5 pxl for the blue and for the red domain respectively. Therefore the extraction width is usually 7 pxl for the blue domain and 9 pxl for the red, to contain most of the signal. The program integrates the extracted signal above the baseline defined by the mean value of the signal at the adjacent interorder positions. Two data tables contain wavelengths and pixel positions of all significant emission lines for each order of a thorium reference spectrum. Starting from guessed positions read in the tables, the program finds the exact positions and automatically deduces for each order the

[1] Munich Image Data Analysis System, European Southern Observatory.

[2] Image Reduction and Analysis Facility, National Optical Astronomy Observatories.

Table 5. IUE observations

Star	JD-2400000.	LWP	Exp. T (m)
HD 2928	50031.973	31681	300
HD 3940	50009.176	31605	105
HD 5776	50013.217	31615	200
HD 12953	46698.362	9167	037
	46705.213	9224	037
	46714.169	9290	037
	46722.172	9350	037
	46729.196	9407	037
HD 13476	49664.225	29471	083
HD 13744	50005.497	31590	150
HD 14433	46698.273	9166	072
	46705.272	9225	042
	46714.224	9291	035
HD 14535	49664.114	29470	120
HD 15316	49664.031	29469	075
HD 16778	50007.065	31602	170
HD 17378	46698.421	9168	040
HD 20041	49663.985	29468	020
HD 21389	46698.231	9165	008
	46705.331	9226	008
	46714.278	9292	008
	46722.133	9349	010
	46729.148	9406	010
HD 46300	46698.143	9163	005
	46714.114	9289	004
	46722.076	9348	004
	46729.086	9405	004
HD 59612	46698.185	9164	030
	48596.899	21952	020
HD 87737	48577.184	21753	005
	48583.044	21808	001
	48588.976	21871	001
	48589.272	21876	001
	48596.995	21954	001
	48612.076	22044	001
HD 100198	49480.707	28096	040
HD 100826	49480.667	28095	023
HD 102878	49480.762	28097	023
HD 103516	49480.549	28093	030
HD 104035	49480.513	28092	015
HD 104111	49480.596	28094	060
HD 161912	49481.474	28091	005
HD 207673	50032.235	31682	050
HD 210221	48612.188	22046	017
HD 211971	48583.083	21809	045
HD 212593	48589.235	21875	005
	48597.035	21955	004
HD 213470	49700.159	29702	057

Table 6. Interstellar components used for wavelength calibration

Ion	Mult.	λ (Å)
Fe II	3	2343.495
Fe II	2	2366.864
		2373.733
		2382.034
Fe II	1	2585.876
		2599.395
Mn II	1	2576.107
		2593.731
		2605.697
Mg II	1	2795.523
	1	2802.698
Mg I	1	2852.120

coefficients of the 3rd order polynomial giving the wavelength calibration.

3.2. UV data

3.2.1. Observations

The stars observed with the IUE satellite are all the A-supergiants in the 1986 IUE Archive, studied before by Talavera & Gómez de Castro (1987), as well as the new set observed by us in campaigns during 1986, 1991, 1994 and 1995. The new spectra were taken using the prime camera of the long-wavelength IUE spectrograph (LWP) in high-resolution mode. The spectral range observed with this configuration is from 1900 Å to 3200 Å with a resolution of $\sim$ 0.2 Å; the most prominent indicators of wind in A-supergiants, Mg II and Fe II lines, are observed in this range.

The IUE observations carried out by us are summarized in Table 5. For each star the date of observation, the image number and the exposure time are provided.

3.2.2. Reduction

All IUE data have been processed at VILSPA using the IUE Spectral Image Processing System (IUESIPS). IUESIPS produces data as free as possible from instrumental effects. These include geometric distortion correction, photometric nonlinearity correction, spectral order extraction and wavelength and flux calibration.

The standard IUE data reduction has an uncertainty in the zero of the wavelength scale which can amount up to 0.5 Å. To correct for this we have measured the observed wavelength of some selected interstellar lines listed in Table 6 and compared with their laboratory wavelength. This method cannot be used in some stars for which the lines selected are not clearly interstellar (lines wider than the IUE instrumental profile). In such a case we compared

Table 7. Visible lines selected for this atlas

Ion	λ (Å)	log gf	E_i(cm^{-1})	j_i	Config$_i$	E_f(cm^{-1})	j_f	Config$_f$
Hα	6562.80	0.7098	82259	(1/2, 3/2)	2p ^{2}P^0	97492	(3/2,5/2)	3d ^{2}D
Hβ	4861.32	−0.0202	82259	(1/2, 3/2)	2p ^{2}P^0	102824	(3/2, 5/2)	4d ^{2}D
Hγ	4340.46	−0.4469	82259	(1/2, 3/2)	2p ^{2}P^0	105292	(3/2, 5/2)	5d ^{2}D
Hδ	4101.73	−0.7527	82259	(1/2, 3/2)	2p ^{2}P^0	106632	(3/2, 5/2)	6d ^{2}D
Hϵ	3970.07	−0.9929	82259	(1/2, 3/2)	2p ^{2}P^0	107440	(3/2, 5/2)	7d ^{2}D
He I	5875.7	0.739	169087	(2,1,0)	2p ^{3}P^0	186102	(3,2,1)	3d ^{3}D
	4471.5	0.052	169087	(2,1,0)	2p ^{3}P^0	191445	(3,2,1)	4d ^{3}D
Na I	5895.92	−0.184	0	1/2	3s ^{2}S	16956	1/2	3p ^{2}P^0
	5889.95	0.117	0	1/2	3s ^{2}S	16968	3/2	3p ^{2}P^0
Ca II	3968.47	−0.162	0	1/2	4s ^{2}S	25192	1/2	4p ^{2}P^0
	3933.66	0.140	0	1/2	4s ^{2}S	25414	3/2	4p ^{2}P^0
Mg II	4481.2	0.978	71491	(5/2, 3/2)	3d ^{2}D	93800	(5/2, 7/2)	4f ^{2}F^0

the observed spectrum with that of HD 46300 which shows several narrow lines, and henceforth can be used as a reliable template.

Finally, the lines have been normalized to a nearby continuum; we have selected the same continuum windows as Talavera & Gómez de Castro (1987).

4. The spectral atlas

The lines studied in this work have been selected because:

1. Either they are good tracers of winds and mass outflow. For instance not all the UV lines obtained in the 1900 − 3200 Å range with IUE are represented. We have selected a sub-sample based on the previous work of Talavera & Gómez de Castro (1987).

2. Or they are useful spectroscopic indicators for the determination of stellar parameters: effective temperature, gravity and rotational velocity.

The selected lines are listed in Table 7 (visible) and Table 8 (ultraviolet) together with their basic atomic parameters. For the ultraviolet lines, the atomic data come from the semi-empirical calculations of Kurucz & Peytremann (1975).

The atlas, which is accesible from the CDS via ftp, is presented in a comprehensible way by means of two different kind of plots. The spectral atlas of stars with visible spectra only is presented with three stars per page. The line profiles of each star are represented in 7 different panels. These plots are designated collectively as Fig. 1. The spectral atlas of stars with both visible and IUE spectra or with IUE spectra only is presented with one star per page. All the line profiles corresponding to the same star are displayed in 12 different panels within the same page. These plots are designated collectively as Fig. 2. We provide the HD/BD number, the spectral type and the absolute visual magnitude for each star.

The profiles (normalized to the nearby continuum) are plotted versus wavelength (in Å). The visible lines are displayed in the first seven panels corresponding to: the lines of H I Balmer series, He I and Mg II and the doublet lines of Ca II and Na I. The ultraviolet lines are shown in bottom panels: Mg II (uv1) and Fe II (uv1, uv2, uv3, uv62, uv63, uv161). The laboratory wavelengths of the lines are marked by a dashed vertical line. Empty panels indicate that there are no observations at this wavelength range for a given star.

The flux scale varies from source to source to better display the observed profiles. We have selected for each star the best quality spectra obtained (best S/N ratio and spectral resolution) of all these available from the different campaigns. The IUE spectra are often very noisy, especially at the shortest wavelength. Where that was the case we smoothed the spectrum with a boxcar of two, three or five points in order to show a decent profile.

We have observed most of the stars several times in various spectral ranges to study their variability. Variations have been detected in Hα, Mg II (uv1) and Fe II (uv1, uv62, uv63). No evidence of variability has been detected in the other lines. We have represented in Fig. 3 a summary of this study. Figure 3 is presented in the form of a single plot for each star containing two or more spectra. The spectra are labeled with the date of observation and with the HD/BD number of the star. All the Hα profiles are displayed for each variable A-supergiant. We have also selected some few representative examples of variations in the UV range. As in Fig. 1 the laboratory wavelength of the lines is marked.

5. Results

Our findings can be summarized as follows:

H I.- The Hα line is shown to be the most sensitive visible indicator of stellar winds in A-type supergiants. The profiles vary from pure symmetric absorption in the less luminous stars to variable emission profiles in some sources. As noted by Rosendhal (1973) the influence of luminosity upon the shape of Hα follows a clear trend: as

Table 8. Ultraviolet lines selected for this atlas

Ion	λ (Å)	log gf	E_i(cm^{-1})	j_i	Config$_i$	$E_{\rm f}$(cm^{-1})	$j_{\rm f}$	Config$_{\rm f}$
Mg II (1)	2802.70	−0.203	0.000	1/2	3s ^{2}S	35669.310	1/2	3p ^{2}P^0
	2795.53	0.098	0.000	1/2	3s ^{2}S	35760.880	3/2	3p ^{2}P^0
Fe II (63)	2772.719	−1.533	8391.938	5/2	a ^{4}D	44446.878	7/2	z ^{4}D^0
	2768.940	−0.971	8680.454	3/2	a ^{4}D	44784.761	5/2	z ^{4}D^0
	2761.813	−0.898	8846.768	1/2	a ^{4}D	45044.168	3/2	z ^{4}D^0
	2749.482	−0.581	8846.768	1/2	a ^{4}D	45206.450	1/2	z ^{4}D^0
	2749.182	−0.281	8680.454	3/2	a ^{4}D	45044.168	3/2	z ^{4}D^0
	2746.978	0.055	8391.938	5/2	a ^{4}D	44784.761	5/2	z ^{4}D^0
	2739.545	0.331	7955.299	7/2	a ^{4}D	44446.878	7/2	z ^{4}D^0
	2736.968	−0.545	8680.454	3/2	a ^{4}D	45206.450	1/2	z ^{4}D^0
	2727.538	−0.349	8391.938	5/2	a ^{4}D	45044.168	3/2	z ^{4}D^0
	2714.414	−0.398	7955.299	7/2	a ^{4}D	44784.761	5/2	z ^{4}D^0
Fe II (62)	2755.733	0.425	7955.299	7/2	a ^{4}D	44232.512	9/2	z ^{4}F^0
	2749.324	0.323	8391.938	5/2	a ^{4}D	44753.799	7/2	z ^{4}F^0
	2746.487	0.163	8680.454	3/2	a ^{4}D	45079.879	5/2	z ^{4}F^0
	2743.196	−0.050	8846.768	1/2	a ^{4}D	45289.801	3/2	z ^{4}F^0
	2730.735	−0.712	8680.454	3/2	a ^{4}D	45289.801	3/2	z ^{4}F^0
	2724.879	−0.800	8391.938	5/2	a ^{4}D	45079.879	5/2	z ^{4}F^0
	2716.683	−1.484	7955.299	7/2	a ^{4}D	44753.799	7/2	z ^{4}F^0
	2709.373	−2.858	8391.938	5/2	a ^{4}D	45289.801	3/2	z ^{4}F^0
	2692.826	−3.239	7955.299	7/2	a ^{4}D	45079.879	5/2	z ^{4}F^0
Fe II (1)	2631.321	−0.274	667.683	5/2	a ^{6}D	38660.043	7/2	z ^{6}D^0
	2631.045	−0.271	862.613	3/2	a ^{6}D	38858.958	5/2	z ^{6}D^0
	2628.291	−0.425	977.053	1/2	a ^{6}D	39013.206	3/2	z ^{6}D^0
	2625.664	−0.435	384.790	7/2	a ^{6}D	38458.981	9/2	z ^{6}D^0
	2621.669	−0.930	977.053	1/2	a ^{6}D	39109.307	1/2	z ^{6}D^0
	2620.408	−1.801	862.613	3/2	a ^{6}D	39013.206	3/2	z ^{6}D^0
	2617.618	−0.508	667.683	5/2	a ^{6}D	38858.958	5/2	z ^{6}D^0
	2613.820	−0.322	862.613	3/2	a ^{6}D	39109.307	1/2	z ^{6}D^0
	2611.873	0.032	384.790	7/2	a ^{6}D	38660.043	7/2	z ^{6}D^0
	2607.086	−0.099	667.683	5/2	a ^{6}D	39013.206	3/2	z ^{6}D^0
	2599.395	0.417	0.000	9/2	a ^{6}D	38458.981	9/2	z ^{6}D^0
	2598.369	−0.029	384.790	7/2	a ^{6}D	38858.958	5/2	z ^{6}D^0
	2585.876	−0.116	0.000	9/2	a ^{6}D	38660.043	7/2	z ^{6}D^0
Fe II (161)	2498.897	0.365	21581.638	9/2	a ^{4}H	61587.214	11/2	z ^{4}I^0
Fe II (2)	2413.308	−0.397	977.053	1/2	a ^{6}D	42401.302	3/2	z ^{6}F^0
	2411.062	−0.327	977.053	1/2	a ^{6}D	42439.822	1/2	z ^{6}F^0
	2410.521	−0.033	862.613	3/2	a ^{6}D	42334.822	5/2	z ^{6}F^0
	2406.660	−0.175	862.613	3/2	a ^{6}D	42401.302	3/2	z ^{6}F^0
	2404.882	0.201	667.683	5/2	a ^{6}D	42237.033	7/2	z ^{6}F^0
	2404.430	−0.936	862.613	3/2	a ^{6}D	42439.822	1/2	z ^{6}F^0
	2399.242	−0.107	667.683	5/2	a ^{6}D	42334.822	5/2	z ^{6}F^0
	2395.627	0.413	384.790	7/2	a ^{6}D	42114.818	9/2	z ^{6}F^0
	2395.416	−0.992	667.683	5/2	a ^{6}D	42401.302	3/2	z ^{6}F^0
	2388.629	−0.131	384.790	7/2	a ^{6}D	42237.033	7/2	z ^{6}F^0
	2383.060	−1.337	384.790	7/2	a ^{6}D	42334.822	5/2	z ^{6}F^0
	2382.034	0.557	0.000	9/2	a ^{6}D	41968.046	11/2	z ^{6}F^0
	2373.733	−0.469	0.000	9/2	a ^{6}D	42114.818	9/2	z ^{6}F^0
	2366.864	−3.357	0.000	9/2	a ^{6}D	42237.033	7/2	z ^{6}F^0
Fe II (3)	2380.757	−0.628	667.683	5/2	a ^{6}D	42658.224	7/2	z ^{6}P^0
	2364.825	−0.344	384.790	7/2	a ^{6}D	42658.224	7/2	z ^{6}P^0
	2359.111	−0.542	862.613	3/2	a ^{6}D	43238.586	5/2	z ^{6}P^0
	2348.300	−0.248	667.683	5/2	a ^{6}D	43238.586	5/2	z ^{6}P^0
	2344.278	−0.450	977.053	1/2	a ^{6}D	43620.957	3/2	z ^{6}P^0
	2343.495	0.112	0.000	9/2	a ^{6}D	42658.224	7/2	z ^{6}P^0
	2338.008	−0.385	862.613	3/2	a ^{6}D	43620.957	3/2	z ^{6}P^0
	2332.798	−0.191	384.790	7/2	a ^{6}D	43238.586	5/2	z ^{6}P^0
	2327.391	−0.631	667.683	5/2	a ^{6}D	43620.957	3/2	z ^{6}P^0

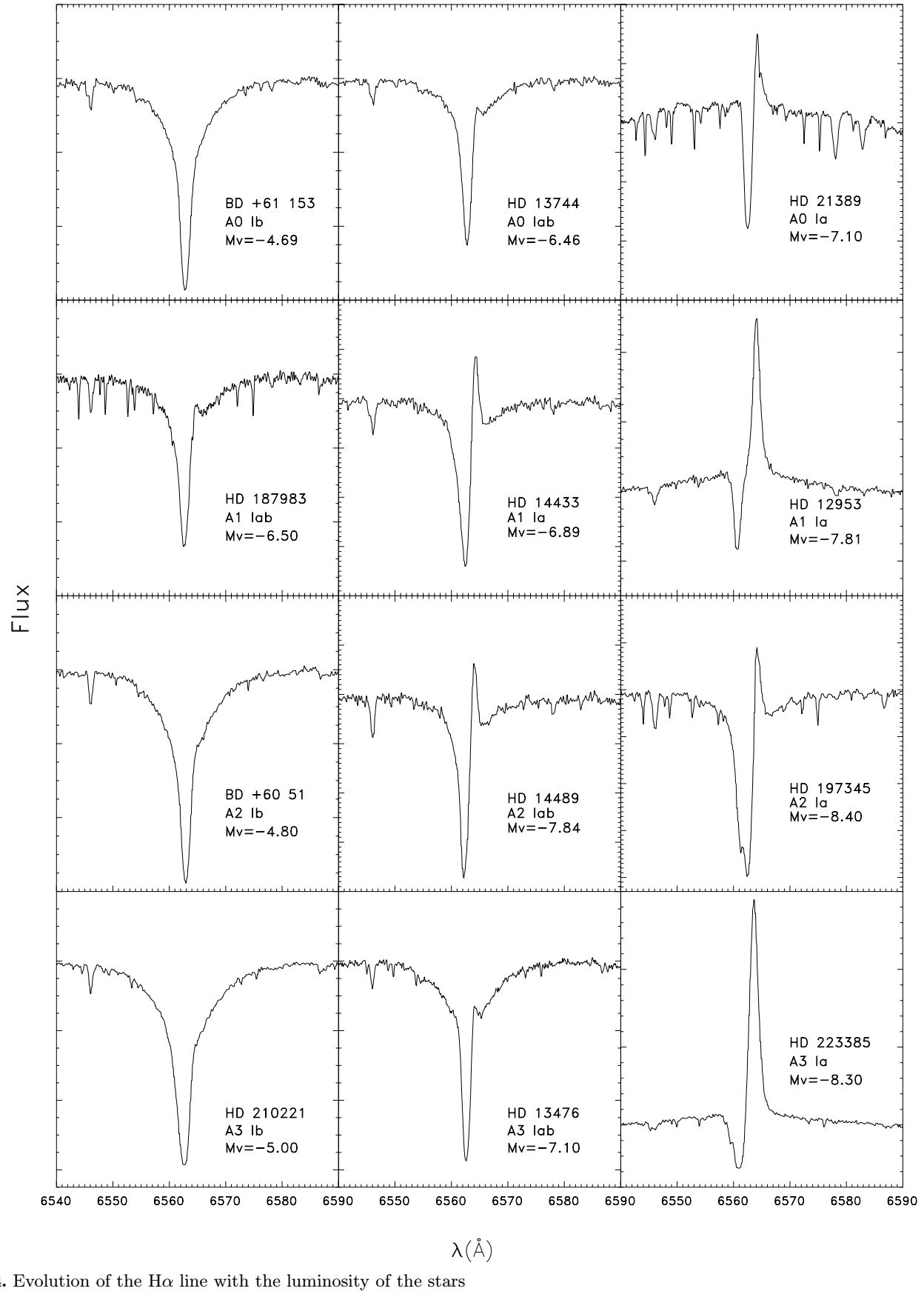

Fig. 4. Evolution of the Hα line with the luminosity of the stars

the luminosity increases the initially symmetric absorption profiles become asymmetric with the violet wing being more extended than the red one up to a point in which a significant emission becomes visible and then the strength of this emission component increases steadily with the luminosity. This behaviour is particularly clear for stars with the same spectral type as it is well illustrated in Fig. 4.

Variations in Hα are observed in most of the A-supergiants. Hβ presents a symmetric absorption profile in all the A-supergiants except in HD 12953, HD 14535, HD21389, HD 223960 and HD 223385. The only star that shows any indication of asymmetry in Hγ and Hδ is HD 223960. These stars also display the strongest variations in Hα.

Ca II, Mg II (4481 Å), Na I and He I.- These lines are photospheric (symmetric absorption profiles) in all sources, no wind effects have been detected. The Ca II (H and K) and Na I D lines are strongly contaminated by the contribution from interstellar clouds. The line profiles show a complex structure with multiple components formed in absorbing regions at different velocities along the line of sight.

Mg II.- The UV resonance lines of Mg II are well known to be a sensitive indicator of wind in A-supergiants. Talavera & Gómez de Castro (1987) described the profiles and divided A-supergiants into two groups depending on these resonance ultraviolet lines profiles. The less luminous stars did not show wind effects while the luminous ones showed the evidence of mass-loss. Our observations confirm this trend. The most luminous A-supergiants present two different types of profiles characteristic of mass outflow. In some stars the Mg II lines are asymmetric with no emission feature and a sharp blue edge. In other stars the Mg II profiles are composed of several deep shortward shifted components. Variations are observed in many stars but the most spectacular profiles variations are observed in two low-luminosity stars: HD 46300 and HD 87737 where we can see the appearance and evolution of a shortward shifted component superimposed on the profile of the Mg II.

Fe II.- The Fe II spectrum of the stars showing evidence of mass-loss in Hα is characterized by the presence of blue-shifted discrete absorption components. However not all the stars in this group present this behaviour. There are several stars whose Fe II lines are asymmetric and only slightly shortward shifted and other stars which present perfectly symmetric absorption lines. We have searched for variable components in the Fe II lines and we have detected these variations in the spectra of the most luminous stars.

Acknowledgements. We wish to thank Dr. A. Kaufer for having kindly provided unpublished optical data. We also thank the staff at VILSPA, La Palma, Calar Alto and Pic Du Midi observatories for the kind assistance during the observations. This work was partially supported by DGICYT PB93-491.

References

Abbott D.C., 1978, ApJ 225, 893
Achmad L., Lamers H.J.G.L.M., Pasquini L., 1997, A&A 320, 196
Baudrand J., Böhm T., 1992, A&A 259, 711
Bouw G.D., 1981, PASP 93, 45
Cassinelli J.P., Castor J.I., Lamers H.J.G.L.M., 1978, PASP 90, 496
Cananzi K., Augarde R., Lequeux J., 1993, A&AS 101, 599
Fernie J.D., 1983, ApJS 52, 7
Garmany C.D., Stencel R.E., 1992, A&AS 94, 211
Groenewegen M.A.T., Lamers H.J.G.L.M., 1991, A&A 243, 249
Hensberge H., Lamers H.J.G.L.M, de Loore C., Bruhweiler F.C., 1982, A&A 106, 137
Humphreys R.M., 1978, ApJS 38, 309
Kaltcheva N.T., Georgiev L.N., 1994, MNRAS 269, 289
Kunasz P.B., Morrison N.D., 1982, ApJ 263, 226
Kurucz R.L., Peytremann E., 1975, Smithsonian Astrophys., Obs. Spec. Rept. No. 362.
Kudritzki R.P., Springmann U., Puls J., Pauldrach A.W.A., Lennon M., 1997, in 2nd Boulder-Munich Workshop, ASP Conf., I. Howarth (ed.), p. 131
Lamers H.J.G.L.M., Snow T.P., Lindholm D.M., 1995, ApJ 455, 269
Lamers H.J.G.L.M., Stalio R., Kondo Y., 1978, ApJ 223, 207
Lamers H.J.G.L.M., Snow T.P., 1978, ApJ 219, 504
McCarthy J.K., Kudritzki R.P., Lennon D.J., Venn K.A., Puls J., 1997, ApJ 482, 757
Middelburg F., 1981, IHAP Users Manual
Owocki S.P., 1992, in The Atmospheres of Early Type Stars, U. Heber & C.S. Jeffery (eds.). Berlin: Springer-Verlag, p. 393
Praderie F., Talavera A., Lamers H.J.G.L.M., 1980, A&A 86, 271
Rosendhal J.D., 1973, ApJ 186, 909
Stothers R.B., 1991, ApJ 383, 820
Talavera A., Gómez de Castro A.I., 1987, A&A 181, 300
Underhill A.B., Doazan V., 1982, B stars with and without emission lines, NASA SP-456
Verdugo E., Talavera A., Gómez de Castro A.I., 1999, A&A (in press) (Paper II)